Photochemical reactivity of phenyl (methyl-tetrazolyl) ketone – hydrogen atom transfer vs. electron transfer

Maxime Fréneau, Corentin Lefebvre, Mario Andrés Gómez Fernández, Claire Richard, Norbert Hoffmann

Photochemical reactivity of phenyl (methyl)tetrazolium ketone- Hydrogen atom transfer *vs* electron transfer

Maxime Fréneau[1,2], Corentin Lefebvre[2], Mario Andrés Gomez Fernandez[2], Claire Richard[1]*, Norbert Hoffmann[2]*

[1] Université Clermont Auvergne, CNRS, SIGMA Clermont, ICCF, F-63000 Clermont-Ferrand, France

[2] CNRS, CNRS, Université de Reims Champagne-Ardenne, ICMR, Equipe de Photochimie, UFR Sciences, B.P. 1039, 51687 Reims, France

Abstract:

Phenyl (methyl)tetrazolium ketone (**1**) is a synthesis intermediate of tetrazolyloxime fungicides and can be also generated upon their irradiation. Its photolysis is highly solvent dependent which prompted us to investigate more deeply the reaction mechanism. Nanosecond laser flash photolysis of **1** yielded the triplet excited state (λ_{max} = 390/570 nm) immediately after the pulse. This latter was converted into different secondary species that were identified using their specific reactivity as well as product studies. The ketyl radical (λ_{max} = 315/475 nm) was generated in less than 0.02 μs in a good H-donor solvent such as 2-propanol and in around 0.06 μs in cyclohexane, a medium H-donor solvent. In 2-propanol, ketyl radicals decayed by a second order reaction to yield pinacol (yield 45%) while in cyclohexane, they decayed by a second order reaction in the bulk leading to pinacol (yield 21%) and by recombination with the cyclohexyl radical in the cage in an apparent first order reaction to generate an adduct (yield 10%). In a polar and non H-atom donor solvent as acetonitrile, the zwitterionic diradical (λ_{max} = 460 nm) was formed in 0.6 μs with final formation of an atypic dimer. Thus two mechanisms of hydrogen atom transfer are observed. In polar acetonitrile solvent, a two-step-process occurs where the electron is transferred first and the proton follows. In non-polar 2-propanol and cyclohexane solvents, a one-step process takes place where the electron and the proton are simultaneously transferred.

Key words: Fungicide, laser flash photolysis, ketyl radical, zwitterionic diradical, hydrogen atom transfer, proton coupled electron transfer.

Introduction

Plant protection is a key issue in connection with food supply of the mankind. Due to resistance to existing pesticides and environmental requirements and legislation, an increasing number of chemical compounds are synthesized and tested in this regard. Chemical structures of such compounds become more and more complex. Concomitantly with these developments, the weak stability of highly active compounds becomes a decisive problem. In this context, photostability plays a key role. Often, new highly active compounds loss almost completely their activity when exposed to solar light in field. A deep understanding of the mechanisms of corresponding photochemical reactions is necessary for either suppress or at least reduce these processes or to conceive or design photostable molecules and finally diminish the "chemical impact" of plant protection in the environment.

Recently, we performed a detailed investigation on the photodegradation mechanism of tetrazolyloxime fungicides in order to increase their photostability.[1] In the course of these investigations, we observed the formation of the aromatic ketone **1** (Scheme 1) among other compounds. Compound **1** is also a synthesis intermediate of fungicides such as picarbutrazox (Scheme 1).[2]

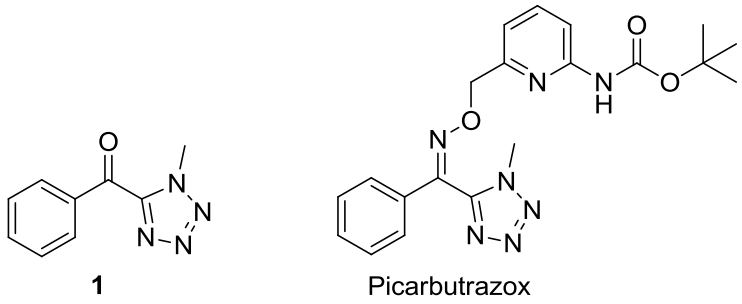

Scheme 1. Chemical structure of **1** and picarbutrazox

We became interested in the photochemical transformations of ketone **1** because of the possibility of hydrogen atom transfer. In fact in such reactions, hydrogen is often transferred according to two mechanisms: Either the electron and the proton are transferred simultaneously (hydrogen atom transfer, HAT) to the electronically excited reaction partner or the electron is transferred first and the proton follows.[3] These two elementary steps are part of a larger ensemble of proton coupled electron transfer processes (PCET).[4,5]

Experimental

General information

Ketone **1** was a gift from Bayer Crop Science. All other reagents were of the highest grade available and used as received. UV-vis spectra were recorded using a Varian Cary 3 spectrophotometer. ^{1}H and ^{13}C NMR spectra were measured in $CDCl_3$ with TMS as an internal standard by using a 600 MHz (^{1}H resonance) a Bruker spectrometer. The identification of photoproducts was performed using High resolution mass spectrometry (HRMS) constituted of an Orbitrap Q-Exactive (Thermoscientific) coupled to an ultra-high performance liquid chromatography (UHPLC) instrument Ultimate 3000 RSLC (Thermoscientific). Analyses were carried out in both negative and positive electrospray modes (ESI^+ and ESI^-). UHPLC separations were performed using a Phenomenex reversed phase column C_{18} grafted silica, (100 mm length, 2.1 mm i.d., 1.7 µm particle size). The binary solvent system used was composed of acetonitrile (MeCN) and water acidified with 0.5‰ v/v formic acid. The gradient program was 5% ACN for the 7 first min, followed by a linear gradient to 99% in 7.5min and kept constant until 20 min. The flow rate was set at 0.45 mL/min and injection volume was 5 µL. Identification of photoproducts was based on structural elucidation of mass spectra and the use of accurate mass determination obtained with the Orbitrap high resolution. HPLC-UV analyses were performed using a NEXERA XR HPLC-DAD apparatus using the same column and the same HPLC conditions as previously indicated.

Laser flash photolysis

Transient absorption experiments were carried outon a nano laser flash photolysis spectrometer from Applied Photophysics (LKS.60) using a frequency-quadrupled Nd:YAG laser (Quanta-Ray GCR-130-1, pulse duration 9 ns). The procedures used for transient absorption spectroscopy measurements have been described previously. [10] The spectral characteristics of **1** are given in Table SI-1 and Figure SI-1. The maximum of absorption is just below 270 nm and **1** was therefore excited at 266 nm. Peroxodisulfate was used as a chemical actinometer.

Steady state irradiations

For preparative purpose, irradiations were conducted in a tube placed in a Rayonet (λ = 300 nm). For quantum yield measurements, solutions were irradiated in parallel beam using a high pressure mercury lamp equipped with an Oriel monochromator. The photon flux was measured using a radiometer QE65000 from Ocean optics. The percentage of **1** conversion was determined by HPLC-UV.

Identification of photoproducts

Photoproduct **2**: Compound **1** (220.5 mg, 1.17 mmol) was dissolved in 30 mL of MeCN, poured in quartz tubes and degassed with argon during 10 min. The tubes were then placed in a Rayonet and irradiated at 300 nm for 40 min. The solvent was evaporated under reduced pressure and the crude was purified by silica column chromatography (petroleum ether/ethyl acetate: 80:20). Starting material was isolated in 58 % yield (150 mg, 0.68 mmol) and product **2** was obtained in 26 % yield (48.3 mg, 0.13 mmol) as a white solid (R_f (petroleum ether/ethyl acetate: 70/30) = 0.22, melting point range : [82.0°C-82.7°C]). NMR ^{1}H (600 MHz, $CDCl_3$, ppm) : δ = 3.74 (s, 3 H), 5.50 (s, 1 H), 5.52 (d, *J* = 14.82 Hz, 1 H), 5.87 (d, *J* = 14.82 Hz, 1 H), 7.19 (m, 3 H), 7.26 (t, *J* = 6.68 Hz, 2 H), 7.54 (t, *J* = 7.82 Hz, 2 H), 7.71 (t, *J* = 7.40 Hz, 1 H), 8.18 (d, *J* = 7.87 Hz, 2 H) ppm. NMR ^{13}C (150 MHz, $CDCl_3$, ppm) : δ = 35.18, 57.12, 73.44, 125.36, 128.87, 129.27, 129.50, 131.45, 134.39, 135.60, 136.48, 151.17, 155.35, 182.44 ppm (Figure SI-2). UHPLC-HRMS: m/z = 377.1463 in ES^+.

Photoproduct **3** in 2-propanol (i-PrOH): Compound **1** (92 mg, 0.49 mmol) was dissolved in 60 mL of i-PrOH, poured in quartz tubes and degassed with argon during 10 min. The tubes are then placed in a Rayonet and irradiated at 300 nm for 4 h. The solvent was evaporated under reduced pressure and the crude was purified by silica column chromatography (petroleum ether/ethyl acetate: 95/5 to 50/50). Product **3** was obtained in 46 % yield (85 mg, 0.22 mmol) as a white solid (R_f (petroleum ether/ethyl acetate: 80/20) = 0.76, brown stain on TLC with vanillin revelator, melting point range : [189.6°C-190.3°C]). NMR ^{1}H (600 MHz, $CDCl_3$, ppm) : δ = 3.89 (s, 3 H), 6.85 (d, *J* = 7.54 Hz, 4 H), 7.07 (s, 2 H), 7.13 (t, *J* = 7.78 Hz, 4 H), 7.25 (t, *J* = 7.40 Hz, 2 H) ppm. NMR ^{13}C (150 MHz, $CDCl_3$, ppm) : δ = 35.55, 79.07, 127.12, 127.45, 128.78, 134.29, 157.70 ppm (Figure SI-3). UHPLC-HRMS: m/z= 379.1618 in ES^+ and 377.1485 in ES^-.

Photoproduct **3** in n-heptane: Compound **1** (96 mg, 0.51 mmol) was dissolved in 110 mL of n-heptane, poured in quartz tubes and degassed with argon during 10 min. The tubes were then placed in a Rayonet and irradiated at 300 nm for 2 h 30. The solvent was evaporated under reduced pressure and the crude was purified by silica column chromatography (petroleum ether/ethyl acetate: 95/5 to 50/50). Product **3** was obtained in 15 % yield (29 mg, 0.08 mmol) as a white solid.

Photoproduct **4**: Compound **1** (220.2 mg, 1.17 mmol) was dissolved in 80 mL of cyclohexane, poured in quartz tubes and degassed with argon during 10 min. The tubes were then place in a Rayonet and irradiated at 300 nm for 6 h. The solvent was evaporated under reduced pressure and the crude was purified by silica column chromatography (petroleum ether/ethyl acetate: 90:10). Stains on TLC

plates were revealed with vanilline. Product **3** was obtained as major product in 21 % yield (94 mg, 0.25 mmol) as a white solid. Minor product **4** was obtained in 10 % yield (31 mg, 0.11 mmol) as a clear liquid (R_f (petroleum ether/ethyl acetate : 80/20) = 0.30, blue stain on TLC with vanillin revelator). NMR ^{1}H (600 MHz, $CDCl_3$, ppm) : δ = 0.99 (qd, *J* = 3.48, 12.42 Hz, 1 H), 1.13 (m, 2 H), 1.24 (m, 2 H), 1.47 (qt, *J* = 3.48, 13.02 Hz, 1 H), 1.70 (m, 2 H), 1.82 (m, 1 H), 2.05 (d, *J* = 12.18 Hz, 1 H), 2.7 (tt, *J* = 2.82, 12.12 Hz, 1 H), 2.85 (s, 1 H), 3.83 (s, 3 H), 7.30 (m, 5 H) ppm. NMR ^{13}C (150 MHz, $CDCl_3$, ppm) : δ = 26.24, 26.29, 26.36, 27.73, 35.72, 46.82, 77.53, 125.43, 127.90, 128.58, 140.32, 157.57 ppm (Figure SI-4). UHPLC-HRMS: m/z= 273.1703 in ES^+.

Results

Product studies

When compound **1** was irradiated in acetonitrile at λ=300 nm, we observed the formation of compound **2**. The reaction was stopped at a conversion of 42% (Scheme 2). Further irradiation led to a very unselective transformation and the complex product mixture could not be characterized. Irradiation of compound **1** in i-PrOH, cyclohexane or n-heptane yielded compound **3**. In cyclohexane, compound **4** was also obtained in small amounts. Formation of compound **3** resembles the well-known photo-pinacolization[6] while the formation of compound **2** is unusual.

Compound **3** results from a reaction in which hydrogen atom transfer plays a central role. In such processes stable ketyl radicals are formed and dimerization leads to pinacol products such as **3**. It must be noted that the best yield of this product is observed when i-PrOH was used as an efficient H-atom donor and as a solvent. In the case of the poor hydrogen atom donor n-heptane, the formation of **3** is much less efficient. In cyclohexane that is a medium hydrogen atom donor, the yield is intermediate. Interestingly, the cyclohexyl radicals resulting from the oxidation of the solvent are able to combine with the ketyl radicals generated from ketone **1** to form compound **4**. The behavior of **1** in MeCN used as a polar solvent with poor hydrogen atom donation properties looks very atypic. The detection of **2** suggests the intermediary formation of a methyl radical and a ketyl radical localized on two different starting molecules. We hypothesized that photochemical electron transfer is involved in the formation of these radicals and of compound **2**.

In order to get a deeper insight into the reaction mechanism, a detailed physico-chemical investigation was performed.

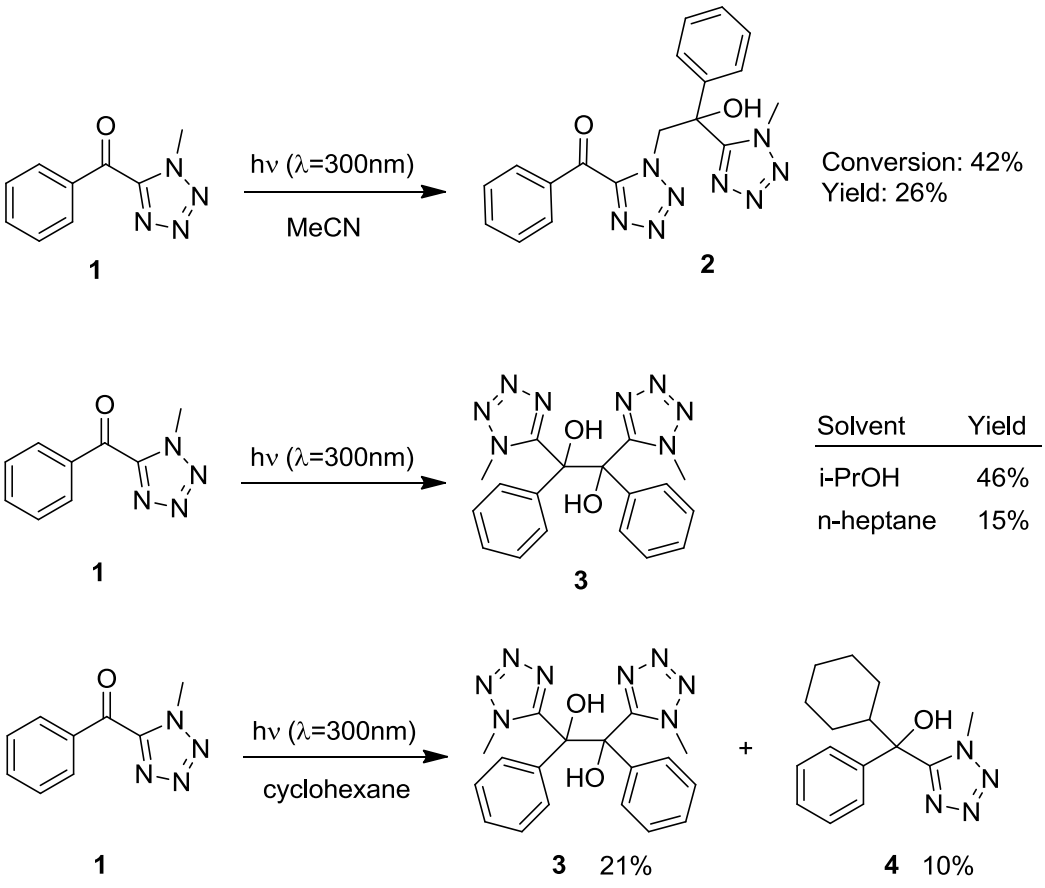

Scheme 2. Photochemical transformations of the aromatic ketone **1**.

Formation of the triplet excited state.

The laser flash photolysis of **1** at 266 nm yielded the same transient species in MeCN, i-PrOH, cyclohexane and n-heptane. It was observed immediately following the laser pulse and showed two maxima at 390 and 570 nm (Figure 1). By plotting the absorbance measured at 380 nm at the end of the pulse against the pulse energy, one got an $\varepsilon\times\Phi$ product of 3300±500 $M^{-1}cm^{-1}$ in cyclohexane and n-heptane, where ε is the molar absorption coefficient of the species at 380 nm and Φ, the quantum yield of the transient formation. The assignment of this transient to the triplet excited state, $^{3}\mathbf{1}^{*}$, was made possible by studying its reactivity with oxygen and anthracene. In MeCN, the lifetime of the transient was reduced by a half upon deoxygenation of the solution (0.34 μs in air-saturated solution against 0.6 μs in argon-saturated solution) demonstrating the scavenging effect of oxygen (Figure 2). Moreover, the irradiation of **1** in the presence of anthracene led to an accelerated decay of the transient at 380 nm and to the formation of the triplet excited state of anthracene well visible at 420 nm (Figure SI-5). This result brings evidence that an energy transfer took place between the transient and ground state anthracene and confirms that the transient was $^{3}\mathbf{1}^{*}$. The quantum yield of $^{3}\mathbf{1}^{*}$ formation was estimated to be equal to 0.26±0.05.

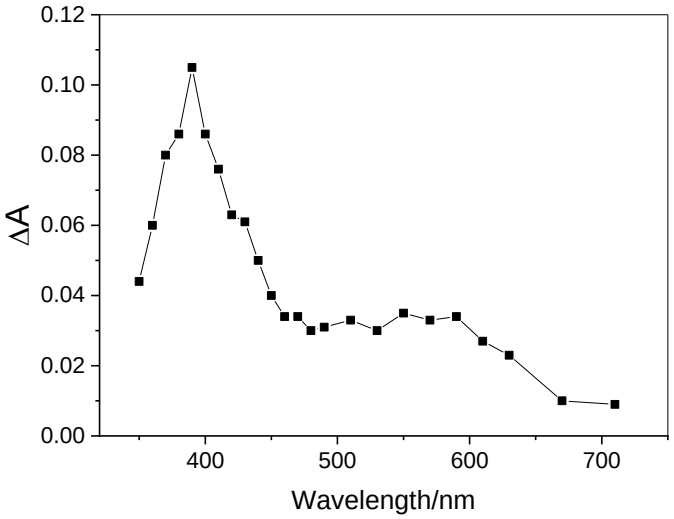

Figure 1 : Transient absorption spectrum measured immediately after the pulse by excitation of **1** at 266 nm in aerated MeCN. (**1**)= 6x10^{-5} M, A_{266} = 0.77

Reactivity of the triplet.

The decay of ^{3}**1*** in deoxygenated medium obeyed an apparent first order kinetics, but was solvent-dependent. As shown in Table 1, the apparent first-order decay rate constant varied in the order MeCN ~ n-heptane < cyclohexane < i-PrOH, i.e. increased with the H-donor capacity of the solvent. In pure i-PrOH, the decay of ^{3}**1*** was too fast to be accurately measured. The rate constant of reaction of ^{3}**1*** with i-PrOH was therefore measured in MeCN/i-PrOH mixtures. From the linear dependence of the apparent first-order decay rate constant on i-PrOH concentration, a value of (4.3±0.4)×10^{6} M^{-1}s^{-1} was obtained (Figure SI-6).

Transient	MeCN	n-heptane	cyclohexane	i-PrOH
Decay rate constant of ^{3}**1***	(1.8±0.2)×10^{6} s^{-1}	(2.0±0.3)×10^{6} s^{-1}	(1.7×10^{7})±0.3 s^{-1}	> 5×10^{7} s^{-1}
Decay rate constant of secondary species	1.7×10^{5} s^{-1} $t_{1/2}$ = 4.1 μs	-	2.5×10^{5} s^{-1} (main process ~80%) 2k/ε_{330}=6.5x10^{5} cm^{-1}s^{-1} (minor process ~20%) $t_{1/2}$ ~ 3.5 μs	2k/ε_{330}=2.7x10^{5} cm^{-1}s^{-1} $t_{1/2}$ ~ 40 μs
Quantum yield of **1** photolysis	0.17±0.03		0.064±0.02	0

Table 1 : Decay rate constants of the transients in deoxygenated solvents and quantum yields of **1** photolysis air air-saturated medium. (**1**)= 6x10^{-5} M

The reactivity of ^{3}**1*** with **1** was also investigated using concentrations of **1** up to 10^{-2} M. In this set of experiments, the solutions were excited at 355 nm to reduce the absorption of solutions. The decay

rate constant of $^3\mathbf{1}^*$ increased linearly with **1** concentration. A bimolecular reaction rate constant of $(9.2\pm0.9)\times10^7\ M^{-1}s^{-1}$ was deduced from the linear plot.

Characterization of the secondary transients.

Secondary species were detected after the decay of $^3\mathbf{1}^*$ in i-PrOH, cyclohexane and MeCN. In MeCN, the growth of the secondary species was slow and kinetically correlated with the decay of $^3\mathbf{1}^*$ (Figure 2). Moreover, the addition of oxygen accelerated the secondary transient formation while reducing the intensity of the signal in accordance with a partial scavenging of $^3\mathbf{1}^*$ by oxygen (Figure 2). This fully confirmed the mother-daughter relationship between the two species. In i-PrOH and cyclohexane, the formation of the secondary transient and the $^3\mathbf{1}^*$ decay were both very fast in agreement with a relationship between the two species (Figure SI-7).

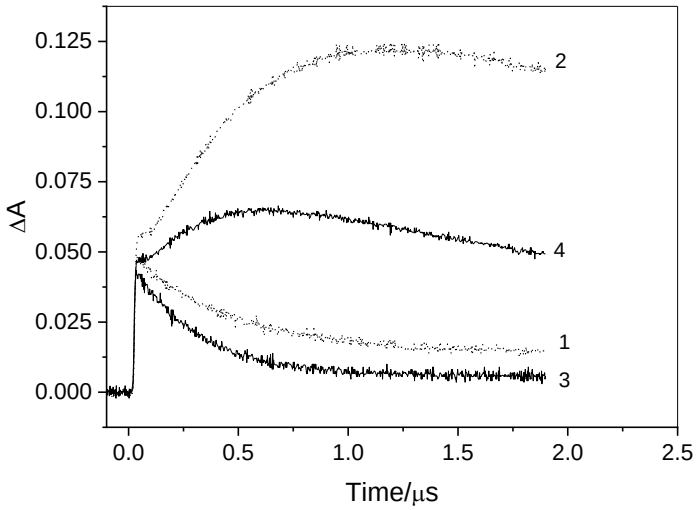

Figure 2: Decay of $^3\mathbf{1}^*$ at 550 nm and growth of the secondary transient at 460 nm. Curves 1 and 2 in deoxygenated MeCN and curves 3 and 4 in air-saturated MeCN. (**1**)= 6×10^{-5} M, A_{266} = 0.77

In i-PrOH and cyclohexane, the secondary species absorption spectra were very similar. They presented two absorption bands with maxima located at 310-320 nm and 470-480 nm. For these two maxima, the intensity of the absorption is twice higher in i-PrOH than in cyclohexane reflecting a more efficient formation in the former solvent. The secondary transient formed in MeCN was different as it showed an absorption band with maximum at 460 nm and no visible other band within the wavelength range 310-350 nm (Figure 3).

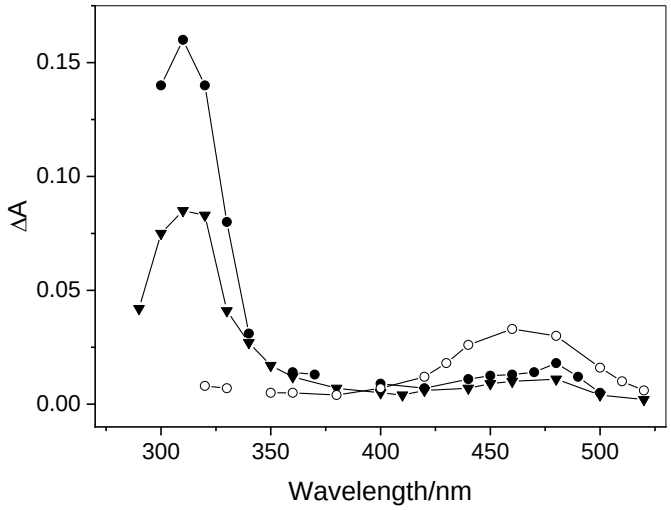

Figure 3: Transient absorption spectra measured by excitation of **1** at 266 nm in argon-saturated i-PrOH (▼), cyclohexane (●), and acetonitrile (○) after the disappearance of $^{3}\mathbf{1}^{*}$: 100 ns following the pulse in i-PrOH, 350 ns in cyclohexane, and 2 μs in MeCN. The other experimental conditions are the same as those in Figure 1.

The lifetimes and reactivities of the secondary species are presented in Table 1. The secondary species formed in i-PrOH and cyclohexane were not detected in air-saturated medium, probably due to a fast quenching by oxygen. In deoxygenated i-PrOH, the secondary species decayed by a second order kinetics with a rate constant equal to $2k/\varepsilon=2.7\times10^{5}$ $cm^{-1}s^{-1}$ at 330 nm (Figure SI-8). Based on these kinetic data, on the formation of pinacol **2** and on the known photoreactivity of benzophenones in i-PrOH, the secondary transient can be assigned to the ketyl radical **A** (Scheme 3).[7]

In deoxygenated cyclohexane, the decay of the ketyl radical was about 10-fold faster than in i-PrOH (Table 1, Figure SI-9). The lower viscosity of cyclohexane compared to i-PrOH (0.98×10^{-3} Pa.s against 2.37×10^{-3} Pa.s at 20°C) can only explain a part of this difference. Indeed, $2k/\varepsilon$ in cyclohexane at 330 nm is expected to be equal to 6.5×10^{5} $cm^{-1}s^{-1}$, i.e. 2.4-fold bigger than in i-PrOH. The fast decay of the ketyl radical in cyclohexane could also be due to a mixture of pseudo-first order and second order kinetics. This is possible if we make the hypothesis that a part of the ketyl radicals **A** react with the cyclohexyl radicals **B**, formed after the H atom abstraction, before escaping the cage. This recombination would be the first order contribution of the decay. It is fully in agreement with the detection of **4**. Once in the bulk, the ketyl radical would decay by a second order kinetics. Such a dual kinetics was nicely described in the photolysis of benzophenone dissolved in soft rubber poly(ethylene-co-butylene) films.[8] By fitting the ketyl radical decay taking $2k/\varepsilon_{330} = 6.5\times10^{5}$ $cm^{-1}s^{-1}$, we obtained that about 80% of the reaction corresponds to the first order geminate recombination in the cage and 20% to the bimolecular recombination in the bulk. When **1** was irradiated in i-PrOH, no geminate recombination was observed. This is in accordance with the literature data that reports the exclusive pinacols formation for benzophenones irradiated in i-PrOH.[9]

The formation of **3** in n-heptane suggests that the ketyl radical **A** is also formed in this solvent. However, we could not observe it at 480 nm. It is probably formed in too small amounts to be detected.

The secondary species formed in MeCN is not the ketyl radical **A** for several reasons. First, its transient absorption spectrum was different from that of the ketyl radical. Moreover, it reacted with oxygen but with a moderate rate constant (2.9×10^7 $M^{-1}s^{-1}$) (Figure SI-10). In deoxygenated medium, it decayed by a clean pseudo-first order kinetics with a rate constant of 1.7×10^5 s^{-1}. The last peculiarity of the secondary transient formed in MeCN is its reactivity with water. A significant enhancement on its decay was measured upon the addition of water (4 and 30%, v/v) (Figure 4) while the ketyl radical was not affected by water in i-PrOH. This result suggests an ionic character for the species and we concluded that it is the zwitterionic diradical.

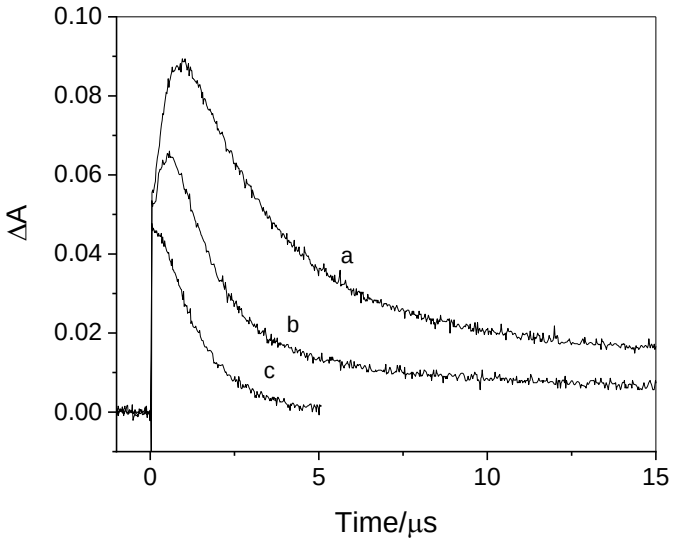

Figure 4 : Decay at 460 nm of the secondary species formed in MeCN in the absence of water (a), in the presence of 4% of water (b), in the presence of 30% of water (c). The other experimental conditions are the same as those in Figure 1.

Mechanisms.

In i-PrOH, the formation of a ketyl radical by H-atom abstraction from i-PrOH is very usual (scheme 3). This is consistent with the known photoreactivity of aromatic carbonyls in H-donor solvents.[10] In the presence of oxygen, the ketyl radical would give the H atom to oxygen[11] and regenerate **1**. This explains the absence of phototransformation of **1** in air-saturated medium (Table 1). In the absence of oxygen, the recombination of two ketyl radicals **A** would lead to pinacol **3**. This pinacolisation is fully in line with the observed second order decay kinetics observed by laser flash photolysis.

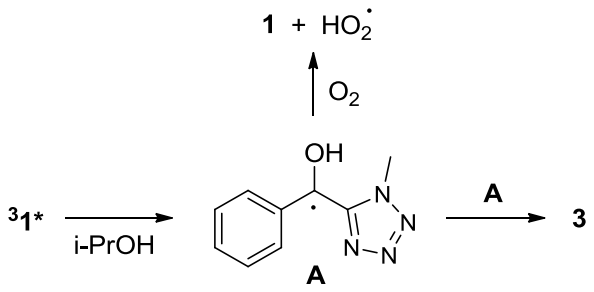

Scheme 3: Formation of pinacol **3** via the ketyl radical **A**

In cyclohexane, the formation of the ketyl radical **A** also takes place as indicated by the formation of pinacol **3** (Scheme 4). The yield is however lower than in i-PrOH, 21% against 46%, in accordance with the existence of competitive reactions, in particular the geminate recombination in the cage of solvent. In such a reaction also compound **4** is formed by combination of a ketyl radical **A** with a cyclohexyl radical **B**.

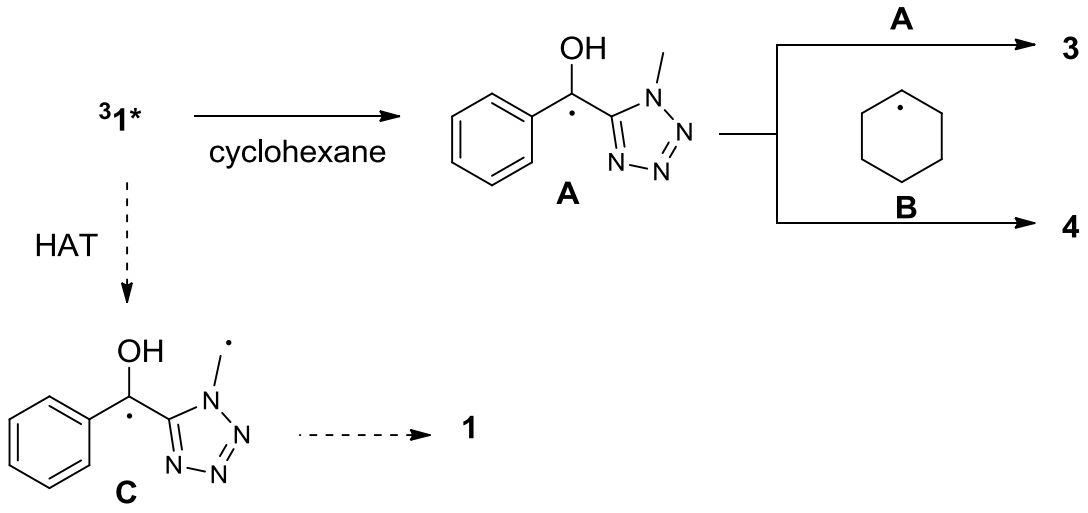

Scheme 4: Formation of pinacol **3** and of the adduct **4** *via* the ketyl radical **A**

In n-heptane, that is a poor H-atom donor solvent, the ketyl radical **A** could not be detected in the laser flash photolysis experiments. Yet, photoproduct **3** was formed in the preparative product studies. These experiments being conducted at a very high **1** concentration, **1** might have been the H-donor, since we demonstrated that a non-negligible reaction between $^{3}\mathbf{1}^{*}$ and **1** can take place. The high **1** concentration used in preparative reactions has probably affected the photoproducts yields. In particular in cyclohexane where the ketyl radical **A** decays by a mixed first order and second order kinetics, increasing **1** concentration is expected to increase the ketyl radical **A** concentration and to favor pinacolisation. Due to the poor H-donor capacity of n-heptane, we initially considered as possible to detect in this solvent the neutral diradical **C** formed through intramolecular H atom transfer.[12] This hypothesis was not confirmed experimentally. Either the reaction does not take place, or this species is too short lived to be detected as shown for other benzophenone derivatives.[11]

In MeCN that is more polar than the other solvents together with a poor H-donor molecule, a very different situation seems to take place. The experimental data are in line with the formation of an ionic intermediary structure that is likely the zwitterionic radical **D** formed by an intramolecular electron transfer (Scheme 5). This assignment is confirmed by the specific reactivity of the secondary species formed in MeCN compared that of ketyl radical **A**.

Under these conditions, we didn't detect a ketyl radical intermediate. As a consequence, we exclude an intermolecular hydrogen transfer from the solvent and suggest an intermolecular hydrogen transfer between the zwitterionic intermediate **D** and **1** at its ground state (Scheme 5). The zwitterionic intermediate **D** can be deprotonated leading to a diradical anion **E** and the protonated ketone $[H\text{-}\mathbf{1}]^{+}$. An electron is then transferred and the neutral radicals **H** and **I** are formed. Radical combination leads to the unusual regioisomer of the coupling product **2**. Alternatively, an electron is transferred first leading to the intermediates **F** and **G**. Proton transfer leads again to the neutral intermediates **H** and **I**. Most probably, the transfer of both particles of the hydrogen atom is coupled (proton coupled electron transfer, PCET). As the intermolecular hydrogen transfer is favored in a polar solvent an increase of the polarity in the transition state of the PCET step is possible. In a corresponding intermolecular step (HAT), the neutral diradical intermediate **C** would be formed as depicted in Scheme 4, this is not the case. Furthermore, it must be pointed out that the one step hydrogen transfer needs a highly structured transition state with highly negative $\Delta S^{\neq}$ values while for the electron transfer in a two-step hydrogen transfer this value is close to zero.[13] The herein described reaction compound **1** leading to the unusual coupling product **2** is therefore directly linked to the formation of the zwitterionic diradical **D**.

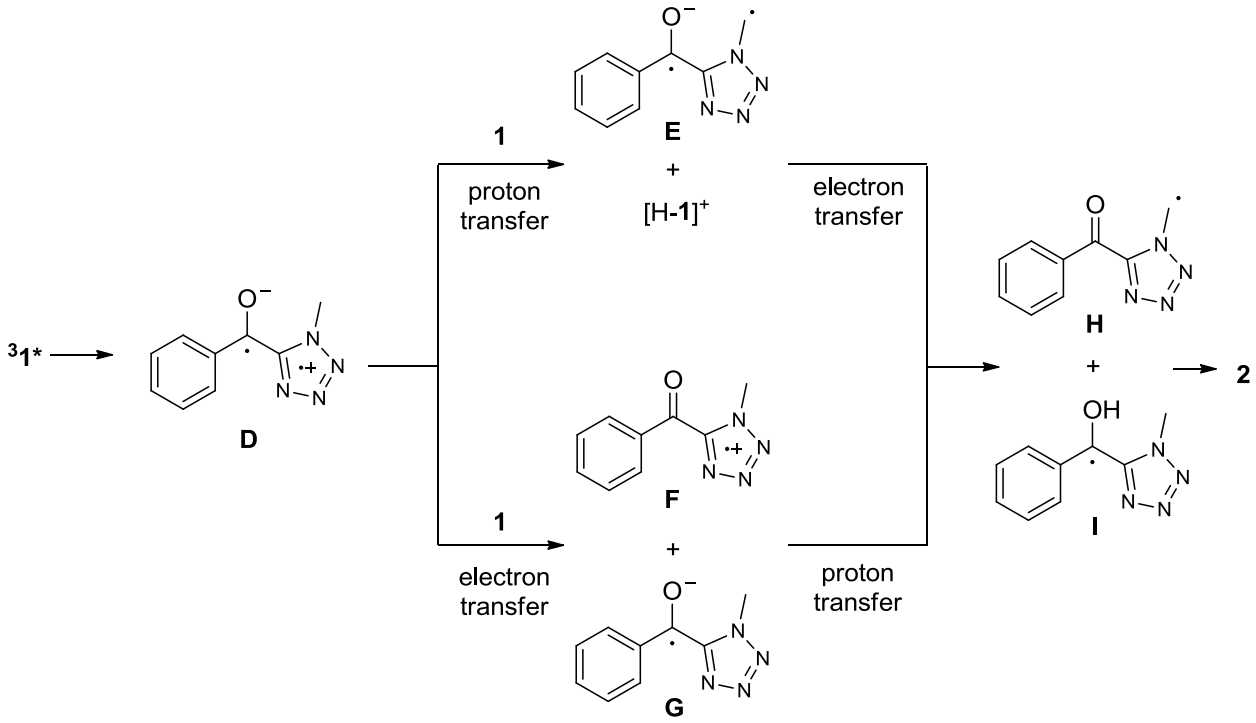

Scheme 5: Formation of dimer **2** *via* the zwitterionic diradical **D** involving proton coupled electron transfer.

Conclusion

The photochemical reactivity of phenyl (methyl)tetrazolium ketone **1** has been studied in detail by means of preparative product studies and laser flash photolysis. When efficient hydrogen atom donor compounds such as isopropanol are used as solvents, ketyl radicals are formed which dimerize leading to photopinacol analogue products as it has previously been reported for aromatic ketones such as benzophenone. A completely different intermediate is formed when ketone **1** is irradiated in acetonitrile. This intermediate possesses a zwitterionic character. A proton coupled electron transfer from this intermediate to **1** at its ground state is suggested to explain the formation of the unusual final product **2**.

…

Acknowledgments

We would like to thank Jye-Shane Yang (National Taiwan University, Taipei) for helpful discussions. We are grateful for financial support from the University of Reims, the French Ministry of Higher Education, Research and Innovation and to Bayer SA (Lyon) for financial support.

…

[1] M. Fréneau, P. de Sainte Claire, N. Hoffmann, J.-P. Vors, J. Geist, M. Euvrard, C. Richard, Phototransformation of Tetrazoline oxime ethers: Photoisomerization vs photodegradation, *RSC Adv.* **2016**, *6*, 5512-5522. M. Fréneau, N. Hoffmann, J.-P. Vors, P. Genix, C. Richard, P. de Sainte Claire, Phototransformation of Tetrazoline Oxime Ethers – Part2: Theoretical Investigation, *RSC Adv.* **2016**, *6*, 63965-63972.

[2] D. Ichinari, A. Nagaki, J. Yoshida, Generation of hazardous methyl azide and its application to the synthesis of key-intermediates of picarbutarox, *Bioorg. Med. Chem.* **2017**, *25*, 6224-6228. T. Kobori, H. Kondo, H. Tsuboi, K. Akiba, A. Koiso, T. Otaguro, H. Nakayama, H. Hamano, A. Ono, T. Asada, Tetrazoyl oxime derivative and agricultural chemical containing the same as active ingredient, *EP 1426371 A1*, 2002

[3] N. Hoffmann, Electron and hydrogen transfer in organic photochemcial reactions, *J. Phys. Org. Chem.* **2015**, *28*, 121-136. N. Hoffmann, Photochemical Electron and Hydrogen Transfer in Organic Synthesis: The control of Selectivity, *Synthesis* **2016**, *48*, 1782-1802.

[4] S. Y. Reece, J. M. Hodgkiss, JA. Stubbe, D. G. Nocera, Photon-coupled electron transfer: the mechanistic underpinning for radical transport and catalysis in biology, *Phil. Trans. R. Soc. B*, **2006**, *361*, 1351-1364. S. Hammes-Schiffer, A. A. Stuchebrukhov, Theory of Coupled Electron and Proton Transfer Reactions, *Chem. Rev.* **2010**, *110*, 6939-6960. D. R. Weinberg, C. J. Galiardi, J. F. Hull, C. F. Murthy, C. A. Kent, B. C. Westlake, A. Paul, D. H. Ess, D. G. McCafferty, T. J. Meyer, Proton-Coupled Electron Transfer, *Chem. Rev.* **2012**, *112*, 4016-4093. A. Migliore, N. F. Polizzi, M. J. Therien, D. N. Beratan, Biochemistry and Theory on Proton-Coupled Electron Transfer, *Chem. Rev.* **2014**, *114*, 3381-3465.

[5] D. C. Miller, K. T. Tarantino, R. R. Knowles, Proton-Coupled Electron Transfer in Organic Synthesis: Fundamentals, Applications, and Opportunities, *Top. Curr. Chem. (Z)* **2016**, *374*, 30, (1-59). N. Hoffmann, Proton-Coupled Electron Transfer in Photoredox Catalytic Reactions, **2017**, *2017*, 1982-1992. J. Ma, X. Zhang, D. L. Phillips, Time-Resolved Spectroscopic Observation and Characterization of Water-Assisted Photoredox Reactions of Selected Aromatic Carbonyl Compounds*, Acc. Chem. Res.* **2019**, *52*, 726-737. E. Fava, M. Nakajima, A. L. P. Nguyen, M. Rueping, Photoredox-Catalyzed Ketyl-Olefin Coupling for the Synthesis of Substituted Chromanols, *J. Org. Chem.* **2016**, *81*, 6959-6964.

[6] M. B. Rubin, Photoinduced Intermolecular Hydrogen Abstraction Reactions of Ketones, In *CRC Handbook of Organic Photochemistry and Photobiology* (W. M. Horspool, P. S. Song, Eds.), CRC Press, Boca Raton, 1995, P. 430.

[7] N. J. Turro, V. Ramamurthy, J. C. Scaiano, Modern Molecular Photochemistry of Organic Molecules, University Science Books, Sausalito, 2010, p. 640

[8] P. P. Levin, A. F. Efremkin, I. V. Khudyakov, Kinetics of benzophenone ketyl free radicals recombination in a polymer: reactivity in the polymer cage vs. reactivity in the polymer bulk**,** *Photochem. Photobiol. Sci.* **2015**, *14*, 891-896.

[9] W. M. Moore, G. S. Hammond, R. P. Foss, Mechnisms of Photoreactions in Solutions. I. Reduction of Benzophenone by Benzhydrol, *J. Am. Chem. Soc.* **1961**, *83*, 2789-2794. J. N. Pitts, R. L. Letsinger, R. P. Taylor, J. M. Patterson, G. Recktenwald, R. B. Martin, Photochemical Reactions of Benzophenone in Alcohols *J. Am. Chem. Soc.* **1959**, *81*, 1068-1077.

[10] F. Bonnichon, C. Richard, Phototransformation of 3-hydroxybenzonitrile in water, *J. Photochem. Photobiol. A* **1998**, *119*, 25–32.

[11] J. C. Scaiano, Laser Flash Photolysis Studies of the Reactions of Some 1,4-Biradicals, *Acc. Chem. Res.* **1982**, *15*, 252-258.

[12] This reaction step would be related to the reactions of o-tolylphenyl ketone and similar derivatives: P. G. Sammes, Photoenolization, *Tetrahedron* **1976**, *32*, 405-422.

[13] J. A. Mayer, Understanding Hydrogen Atom Transfer: From Bond Strengths to Marcus Theory, *Acc. Chem. Res.* **2011**, *44*, 36-46. J. Jung, S. Kim, Y.-M. Lee, W. Nam, S. Fukuzumi, Switchover of the Mechanism between Electron Transfer and Hydrogen-Atom Transfer for a Protonated Manganese(IV)-Oxo Complex by Changing Only the Reaction Temperature, *Angew. Chem. Int. Ed.* **2016**, *55*, 7450-7454.